Signature of an intrinsic point defect in GaN_xAs_{1-x}

N. Q. Thinh, I. A. Buyanova, P. N. Hai, and W. M. Chen
Department of Physics and Measurement Technology, Linköping University, S-581 83 Linköping, Sweden

H. P. Xin and C. W. Tu
Department of Electrical and Computer Engineering, University of California, La Jolla, California 92093
(Received 7 September 2000; published 2 January 2001)

The first experimental signature of an intrinsic defect in GaNAs is provided from an optically detected magnetic resonance study. The resolved central hyperfine structure identifies the defect with a nuclear spin $I = 3/2$, containing either an As_{Ga} antisite or a Ga interstitial. From the strength of the hyperfine interaction and the growth conditions, a complex involving the As_{Ga} antisite seems to be a more likely candidate.

DOI: 10.1103/PhysRevB.63.033203 PACS number(s): 76.70.Hb, 71.55.Eq, 61.72.Ji

Intrinsic point defects in semiconductors have been a subject of extensive research over the past decades, not only because of their high interest as fundamental building blocks of defects, but also due to their important role in materials properties and device performance. Though significant progress has been made in the understanding of some classes of defects, e.g., vacancies in silicon[1] and Zn self-interstitial in ZnSe,[2] a majority of intrinsic defects in most semiconductors are still eluded from a firm grasp of their properties in particular concerning their chemical nature and microscopic structure. This is particularly true for new materials and quantum structures that have only been possible to acquire very recently by modern epitaxial growth techniques. Among the typical representatives are the artificial *N*-containing III-V alloys such as GaNAs. Though this new material system is known to exhibit intriguing fundamental properties such as the giant bandgap bowing,[3–9] that has attracted much interest in potential application for near infrared photonic devices, practically nothing is known about point defects in the material.

In this paper, we shall provide the first experimental signature of an intrinsic defect in GaNAs with a low *N* composition. The characteristic hyperfine structure has been obtained by the optically detected magnetic resonance (ODMR) technique, which reveals a nuclear spin $I = 3/2$ of the defect atom and can be attributed to either an As_{Ga} antisite or a Ga_i interstitial. Based on the knowledge gained from earlier studies of the defect formation and hyperfine interaction of similar defects in the parental compound GaAs, a complex defect involving the As_{Ga} antisite is argued to be a more likely candidate. The highly localized wave function of the unpaired electron at the defect shows that it is a deep-level defect.

All the investigated samples were undoped and were grown at 420 °C, on semi-insulating GaAs substrates by gas source molecular beam epitaxy (MBE). Two types of sample structures were studied: (a) 7 periods $GaAs/GaN_xAs_{1-x}$ (200 Å/70 Å) multiple quantum well (MQW) structures and (b) 1100 Å-thick GaN_xAs_{1-x} epilayers. All samples were started with a 2500 Å -thick GaAs buffer and were finished with a 100-Å thick GaAs cap layer. The *N* composition *x* in the structures was varied from 1.2% up to 2.8%. In both photoluminescence (PL) and ODMR experiments, the UV lines at 333 nm (3.723 eV) or 351 nm (3.532 eV) or the visible 514 nm (2.412 eV) line of an Ar^+ ion laser were used as the above GaAs bandgap excitation source and a tunable cw Ti:sapphire solid state laser as the below GaAs bandgap excitation source. The PL emissions were dispersed using a double grating monochromator and detected by a cooled Ge detector. ODMR experiments were done at around 5 K in a modified Bruker ESR spectrometer working at the *X*-band (9.22 GHz) and in a 95 GHz ODMR system with the aid of an Oxford split-coil 5T magnet. Color filters were used to select the desired spectral range of detection in the ODMR experiments.

Upon the below GaAs bandgap optical excitation, the PL spectrum shows two distinct features as shown in Fig. 1. The first feature is due to the excitonic transitions near the GaNAs bandgap energy. The second feature of unknown origin peaks at a lower energy near 0.85 eV. These two PL emissions have been shown to arise from the GaNAs layers from earlier studies.[10,11] None of these PL emissions is directly related to the defect under study. They merely provided a medium in the ODMR experiments to detect the defect that

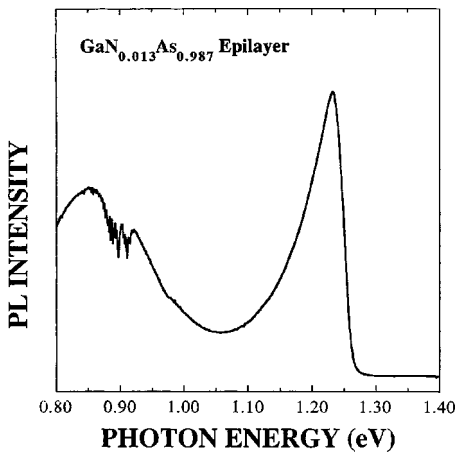

FIG. 1. A representative photoluminescence spectrum from the GaNAs epilayers and the GaNAs/GaAs MQW studied in this work. The particular spectrum was obtained at 2 K from the GaNAs/GaAs epilayer with an *N* composition of 1.3%, with the below GaAs bandgap excitation at 1.442 eV. The structure near 0.9 eV is caused by water absorption in the air.

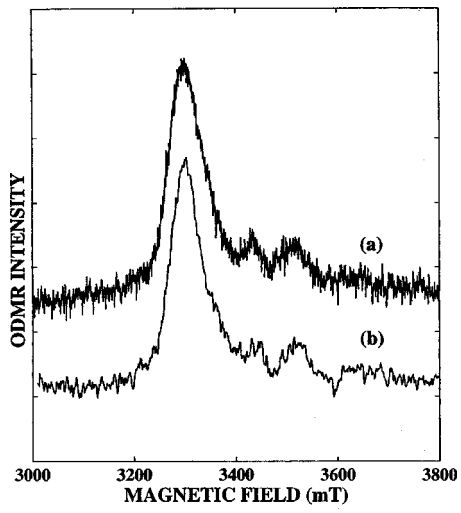

FIG. 2. Typical ODMR spectra obtained at 4.8 K with (a) the above GaAs bandgap excitation (at 3.723 eV) and (b) the below GaAs bandgap excitation (at 1.442 eV), by monitoring the GaNAs PL emissions shown in Fig. 1. The microwave frequency is 94.9 GHz.

is involved in competing recombination channels. Therefore the details of these PL emissions will not discussed here, but can be found in Refs. 10 and 11.

A typical ODMR spectrum is shown in Fig. 2 by monitoring the GaNAs related PL emissions. The fact that the identical ODMR spectrum was obtained with both above and below GaAs bandgap excitation demonstrates that the ODMR signals originate from the GaNAs layers.[12] Detailed ODMR studies at both 95 GHz (Fig. 3) and 9 GHz (Fig. 4) clearly show that the ODMR spectrum contains two parts, a single line at $g=2.03$ (curve b) of unknown origin and a quadruplet (curve c). Both ODMR signals are negative (they are shown positive in the figures just for easy viewing), and correspond to spin-resonance enhanced recombination via the responsible defects that leads to a decrease in PL intensity of the monitored radiative recombination channels.

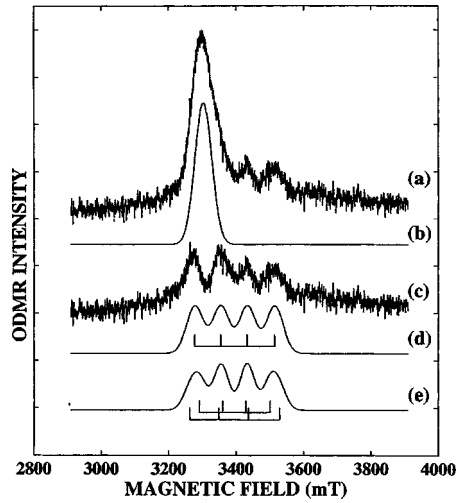

FIG. 3. (a) The GaNAs ODMR spectrum taken at 5 K and 94.9 GHz. (b) The simulated ODMR curve for the single line of $g=2.03$. (c) The quadruplet ODMR spectrum after subtracting the curve b from curve a. (d) The simulated ODMR spectrum for the As_{Ga} antisite with the spin Hamiltonian parameters given in Table I. (e) The simulated ODMR spectrum for the Ga_i interstitial with the spin Hamiltonian parameters given in Table I.

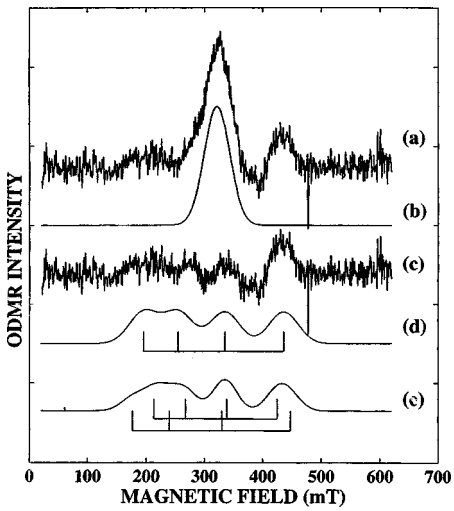

FIG. 4. (a) The GaNAs ODMR spectrum taken at 4.8 K and 9.218 GHz. (b) The simulated ODMR curve for the single line of $g=2.03$. (c) The quadruplet ODMR spectrum after subtracting the curve b from curve a. (d) The simulated ODMR spectrum for the As_{Ga} antisite with the spin Hamiltonian parameters given in Table I. (e) The simulated ODMR spectrum for the Ga_i interstitial with the spin Hamiltonian parameters given in Table I.

The ODMR quadruplet is typical for hyperfine interaction between an unpaired electron spin ($S=1/2$) and a defect nucleus with a nuclear spin $I=3/2$. The ODMR spectrum was found to be isotropic and rather insensitive to the N composition within the range of 1–3 % or to the quantum confinement, i.e., the identical ODMR spectrum was observed in both the GaNAs epilayers and the GaNAs/GaAs MQW. This indicates that the defect state must be a deep level with a very localized wave function. This is also consistent with the observed large and isotropic hyperfine structure resulting from a strong Fermi contact interaction due to a localized state of A_1 symmetry.

Among all the host atoms and possible residual impurities, As (^{75}As with $I=3/2$ and natural abundance of 100%) and Ga (^{69}Ga and ^{71}Ga with natural abundance of 60.1% and 39.9%, respectively, both of $I=3/2$) are the only likely candidates that can be responsible for the characteristic hyperfine structure. Both candidates have been taken into consideration in the analysis of the experimental data with the aid of the following spin Hamiltonian:

$$H=\mu_B \mathbf{B}\cdot\mathbf{g}\cdot\mathbf{S}+\mathbf{S}\cdot\mathbf{A}\cdot\mathbf{I}. \quad (1)$$

Here μ_B is the Bohr magneton, **B** the magnetic field. **g** represents the Zeeman splitting tensor, and **A** denotes the hyperfine interaction tensor. The electron spin is $S=1/2$ and the nuclear spin $I=3/2$. A fairly good fit could be obtained (see Figs. 3 and 4) in both cases when As (curve d) or Ga (curve e) is considered. The determined spin Hamiltonian parameters are listed in Table I.

TABLE I. Spin Hamiltonian parameters obtained for the intrinsic defect studied in this work, from the fit of Eq. (1) to the experimental data. The previously reported results of similar defects are also included for comparison.

Defect	Sample description	Isotropic *g*-tensor	Isotropic *A*-tensor (GHz)	Ref.
The intrinsic defect in GaNAs studied in this work	GaNAs epilayers and GaNAs/GaAs QWs grown by MBE at 420 °C	2.00	2.21(^{75}As) or 1.95(^{69}Ga) 2.48(^{71}Ga)	This work
Earlier results of As_{Ga} antisite	EL2 in LEC as-grown or irradiated GaAs	2.04	2.656(^{75}As)	16
	MBE GaAs grown at 200 °C	2.037	2.691(^{75}As)	17
	MBE GaAs grown at 400 °C	2.03	2.300(^{75}As)	18
Earlier results of Ga_i interstitial	MBE AlGaAs grown at 620 °C	2.025	1.500(^{69}Ga) 1.920(^{71}Ga)	13
	MBE GaAs/AlGaAs superlattices grown at 580 °C	2.007	1.620(^{69}Ga) 2.070(^{71}Ga)	14
	GaAs/AlGaAs heterostructure	2	1.440(^{69}Ga) 1.829(^{71}Ga)	15

In favorable cases of a narrow ODMR linewidth, hyperfine structure from an As atom can be distinctly different from that of a Ga atom. When this occurs, the two isotopes of Ga give rise to two sets of the four-line structure of which the ratios in intensity and in splitting are determined by their ratio in natural abundance and nuclear magnetic moment, respectively.[13–15] The broad linewidth in the present case has, unfortunately, prevented from such a distinction (see curve e in Figs. 3 and 4). Therefore no conclusion can be made on a definite identification of the defect as being due to As or Ga.

However, a close comparison with the previously reported results of similar defects in AlGaAs and the common parental GaAs compound (see Table I)[13–18] can provide a useful clue to whether the involvement of As or Ga is more likely. From Table I, it is clear that the hyperfine interaction deduced for the defect under study seems to be much stronger than that ever reported for a Ga_i interstitial in GaAs and AlGaAs by about 20%.[13–15] This is in sharp contrast to the observations that the hyperfine strength of Ga_i is rather insensitive to the Al composition in AlGaAs.[13] On the other hand, the hyperfine strength, assuming the As atom is responsible, is very close to what has been observed for the As_{Ga} antisite in MBE-GaAs grown at a similarly low temperature (400 °C).[18] This is consistent with the earlier experimental findings that the As_{Ga} antisite can be preferably introduced in GaAs that is grown at low temperature under the off-stoichiometric conditions.[19] Though the exact reason why the hyperfine interaction of the As_{Ga} antisite in MBE-GaAs grown at 200 °C is stronger than that in MBE-GaAs grown at 400 °C is still unclear, it is quite likely that the latter with a weaker hyperfine interaction may arise from a complex involving the As_{Ga} antisite. The complex formation was presumably promoted by an enhanced mobility of atoms at the higher growth temperature. Since the spin density is highly localized at the As_{Ga} antisite (judging from the still rather large hyperfine coupling), the hyperfine structure due to ^{75}As can still remain nearly isotropic, as has been observed from the earlier[16] and the present studies. In the GaNAs alloys, on the other hand, one would expect a strong effect of the nearest neighbors on the hyperfine interaction depending on whether As_{Ga} is surrounded by all As, all *N* or a mixture of two. Though the exact reason is still unknown, the insensitivity in the strength and anisotropy of the hyperfine interaction to the *N* composition seems to be not unexpected for the case dominated by the all As nearest neighbors within the studied range of rather low *N* compositions up to 2.8%. The biaxial strain seems to have little effect on the hyperfine interaction, perhaps because the local crystal field of the defect and the local disorder introduced by *N* are the dominant factor. The latter provides a random field that may have only contributed to the rather broad ODMR linewidth.

Among other possible As- and Ga-related intrinsic point defects, the cation antisites such as Ga_{As} can be ruled out due to their expected non-A_1 symmetry of the state.[20] Very little is so far known of the As_i interstitial in GaAs-based III-Vs. Therefore nothing can be concluded in its role of the defect under study. The fact that it has not been unambiguously observed before in GaAs-based III-Vs by magnetic resonance techniques, however, seems to make it less probable.

In summary, the first signature of an intrinsic defect in GaNAs has been provided from the ODMR studies. The characteristic hyperfine structure consisting of a group of four ODMR lines has identified the involvement of either the As_{Ga} antisite or the Ga_i interstitial in the responsible defect. From a close comparison with the previously published results of the similar defects, a complex involving the As_{Ga} antisite seems to be a more likely candidate. The wave func-

tion of the unpaired electron at the defect is highly localized near the As_{Ga} antisite, explaining the experimental observations that the ^{75}As hyperfine interaction is rather strong and isotropic and is not sensitive to either the *N* composition or the quantum confinement.

The financial support by the Swedish Natural Science Research Council (NFR) and the Swedish Council for Engineering Sciences (TFR) are greatly appreciated. The work at UCSD is partially supported by the National Renewable Energy Laboratory (#AAD-9-18668-07).

[1] G. D. Watkins, in *Deep Centers in Semiconductors*, 2nd ed., edited by S. T. Pantelides (Gordon and Breach Science Publishers, Switzerland, 1992), p. 177.
[2] G. D. Watkins and K. H. Chow, Physica B **273-274**, 7 (1999).
[3] M. Weyers and M. Sato, Appl. Phys. Lett. **62**, 1396 (1992).
[4] M. Kondow, K. Uomi, T. Kitatani, S. Watahiki, and Y. Yazawa, J. Cryst. Growth **164**, 175 (1996).
[5] W. G. Bi and C. W. Tu, Appl. Phys. Lett. **70**, 1608 (1997).
[6] S.-H. Wei and A. Zunger, Phys. Rev. Lett. **76**, 664 (1996).
[7] T. Mattila, S.-H. Wei, and A. Zunger, Phys. Rev. B **60**, R11245 (1999).
[8] J. D. Perkins, A. Mascarenhas, Yong Zhang, J. F. Geisz, D. J. Freidman, J. M. Olson, and S. R. Kurtz, Phys. Rev. Lett. **82**, 3312 (1999).
[9] W. Shan, W. Walukiewicz, J. W. Ager III, E. E. Haller, J. F. Geisz, D. J. Freidman, J. M. Olson, and S. R. Kurtz, Phys. Rev. Lett. **82**, 1221 (1999).
[10] I. A. Buyanova, W. M. Chen, G. Pozina, J. P. Bergman, B. Monemar, H. P. Xin, and C. W. Tu, Appl. Phys. Lett. **75**, 501 (1999).
[11] I. A. Buyanova, W. M. Chen, B. Monemar, H. P. Xin, and C. W. Tu, Appl. Phys. Lett. **75**, 3781 (1999).
[12] Due to the weak ODMR signal and the overlap with a strong, featureless background signal, an estimate of the ODMR signal strength in terms of the total PL intensity was unfortunately not possible at present. What can be said is that the ODMR signal strength is rather similar between that with above and below GaAs bandgap excitation. Please note that the apparent difference between the two curves in Fig. 2 is due to the fact that the curve *b* contains fewer data points as compared to the curve a. Apart from that, the signal-to-noise ratio is rather similar as well.
[13] T. A. Kennedy and M. G. Spencer, Phys. Rev. Lett. **57**, 2690 (1986).
[14] J. M. Trombetta, T. A. Kennedy, W. Tseng, and D. Gammon, Phys. Rev. B **43**, 2458 (1991).
[15] T. Wimbaur, M. S. Brandt, M. W. Bayerl, M. Stutzmann, D. M. Hofmann, Y. Mochizuki, and M. Mizuta, Mat. Sci. Forum **258-263**, 1309 (1997).
[16] For a recent review, see, e.g., F. K. Koschnick and J.-M. Spaeth, Phys. Status Solidi B **216**, 817 (1999).
[17] H.-J. Sun, G. D. Watkins, F. C. Rong, L. Fotiadis, and E. H. Poindexter, Appl. Phys. Lett. **60**, 718 (1992).
[18] K. Krambrock, M. Linde, J.-M. Spaeth, D. C. Look, D. Bliss, and W. Walukiewicz, Semicond. Sci. Technol. **7**, 1037 (1992).
[19] X. Liu, A. Prasad, W. M. Chen, A. Kurpiewski, A. Stoschek, Z. Liliental-Weber, and E. R. Weber, Appl. Phys. Lett. **65**, 3002 (1994).
[20] G. A. Baraff and M. Schulter, Phys. Rev. Lett. **55**, 1327 (1985).